

Corrugated Board Packaging with Innovative Design for Enhanced Durability during Transport

Jędrzej Tworzydło,^a Edyta Piotrowska,^a Rafał Smagacz,^a Damian Mrówczyński ,^b Dariusz Pyś,^c Tomasz Gajewski ,^d and Tomasz Garbowski ,^{e,*}

Laboratory tests were conducted on innovatively designed corrugated board packaging under random vertical vibrations. The innovative designs had reinforced critical corner zones and lid-base interfaces through geometry modifications that increased double-wall regions. A total of 25 packaging variants, differentiated in structure, layer configuration (three-layer and five-layer boards), and surface finish (with and without coatings) were evaluated. The experimental study included box compression tests (BCT) and random vibration tests according to international standards (ISO 12048:1994 and ISO 13355:2016), simulating storage and transportation conditions. All packages were assessed before and after random vibration tests to determine the influence of dynamic loads on structural load-bearing capacity. Unlike previous studies limited to static testing, this work evaluated combined vibration and compression effects under standardized dynamic loading conditions for packaging with relatively low probability of being dropped. Furthermore, it was shown that the innovative design of corrugated board transport packaging presents higher static load capacity after random vibration testing in terms of column compression strength, indicating that no reduction in box strength was observed during simplified transport simulation under pure one-direction dynamic loading. The findings contribute to the optimization of high-durability packaging solutions tailored for the growing demands of complex logistics chains.

DOI: 10.15376/biores.21.1.2229-2253

Keywords: Corrugated board packaging; E-commerce logistics; Transport packaging durability; Mechanical performance; Packaging design optimization; Box compression test; Random vibration testing

Contact information: a: Werner Kenkel Bochnia Spółka z o. o., Adolfa Mitery 7, 32-700 Bochnia; b: Doctoral School, Poznan University of Life Sciences, Wojska Polskiego 28, 60-637 Poznań, Poland; c: Sieć Badawcza Łukasiewicz – Łódzki Instytut Technologiczny, 90-570 Łódź, ul. Marii Skłodowskiej-Curie 19-27, 02-942, Laboratorium Badań Opakowań Transportowych, Warszawa, ul. Konstancińska 11; d: Institute of Structural Analysis, Poznan University of Technology, Piotrowo 5, 60-965 Poznań, Poland; e: Department of Biosystems Engineering, Poznan University of Life Sciences, Wojska Polskiego 50, 60-627 Poznań, Poland; *Corresponding author: tomasz.garbowski@up.poznan.pl

INTRODUCTION

Corrugated board is the foundation of modern packaging, offering an ideal combination of low density, strength, recyclability, and cost-efficiency. With over 80% of global e-commerce shipments relying on corrugated packaging and the global market projected to grow at a 3.7% CAGR by 2032, the importance of this material continues to increase (Market Growth Reports 2023). Its layered construction of fluted medium sandwiched between linerboards makes it highly versatile for diverse product types, from fresh fruits and vegetables to electronics. Sustainability trends drive innovation

(Chowdhury and Kabir 2024), with more than 75% of corrugated fiberboard now being made from recycled content (Market Growth Reports 2023). In addition, manufacturers are integrating features such as water-based coatings, QR-code traceability, and smart packaging sensors to meet circular-economy goals. These forces together motivate the design and testing of advanced corrugated structures tailored for today's fast-growing logistics conditions expectations.

Transport conditions of corrugated board packaging are a critical factor affecting structural integrity, product safety, and the overall quality of goods in transit. During transportation, packaging load-bearing capacity and performance may be affected by factors such as dynamic loads (Mrówczyński *et al.* 2023; Cornaggia *et al.* 2024), pallet overhang (Kim *et al.* 2023a; Mrówczyński *et al.* 2024b), temperature fluctuations, humidity variation (Mrówczyński *et al.* 2024a), and the presence of hand or/and ventilation holes (Fadiji *et al.* 2016; Fadiji *et al.* 2018; Archaviboonyobul *et al.* 2020). For instance, Paternoster *et al.* (2017) showed that combining corrugated board with plastic foil offers superior vibration damping and thermal insulation compared to plastic-only packaging, making it particularly beneficial for temperature- and movement-sensitive goods like beer. In specialized transport, such as for live animals, like day-old chicks, it is crucial to model long-term strength under creep loads to ensure safety and structural reliability throughout the transport window, which typically does not exceed 48 hours (Fehér *et al.* 2023). Kim *et al.* (2023b) showed that optimizing the interaction between pallets and corrugated boxes, such as increasing the stiffness of the pallet's top deck, can allow for the use of lower-grade corrugated board without compromising unit load performance, thereby reducing environmental impact (Kim *et al.* 2023b).

Effective packaging design also requires the inclusion of appropriate safety factors to account for environmental variability, material inconsistencies, and potential structural damage during manufacturing. The importance of these factors increases in the case of extreme transport conditions, such as high humidity or low temperatures, which can significantly reduce the resistance of corrugated board to compression and cracking. Therefore, compliance with FEFCO guidelines and ASTM/ISO standards is essential to ensure high packaging durability and reliability (Garbowski 2023a,b). These findings highlight the need for an interdisciplinary and data-driven approach to the design and evaluation of corrugated transport packaging, especially within complex and extended logistics chains.

Given the significant influence of transport conditions on packaging performance, it becomes equally important to assess how these conditions affect the quality of the transported products themselves, especially in the case of perishable goods. Such products are highly susceptible to damage from shocks and vibrations during transport, which can lead to bruising, softening, and reduced shelf life. Studies have shown that appropriate packaging can considerably reduce such quality losses. For example, Annibal *et al.* (2023) have shown that strawberries packed in single-row mini-trays sustained far less bruising compared to those in plastic crates, due to better vibration damping properties. For the fruit of 'Jiro' persimmons, using modified atmosphere packaging within corrugated board boxes helped preserve fruit firmness and slow down softening during refrigerated overseas shipping (Fahmy and Nakano 2013). Finite element analysis of pears under impact loading revealed that adding a second corrugated board layer reduced stress by over 30%, thereby enhancing product protection (Hafizh *et al.* 2024). Conversely, for figs, corrugated board boxes alone were insufficient under rough transport conditions, resulting in significantly higher mass loss compared to expanded polystyrene alternatives (Çakmak *et al.* 2010).

These results emphasize the necessity of aligning packaging design not only with structural requirements but also with the specific sensitivity of the transported products.

An important factor occurring during transport is vertical vibration, whose prolonged impact can also lead to damage of products and packaging. To analyze and replicate these conditions in the laboratory, a vertical random vibration test is performed using the power spectral density (PSD) method (ISO 13355 2016), which allows for the description of random vibrations in the frequency domain. The PSD approach is widely applied in studies of aircraft structures (Sonnenberg *et al.* 2018), road vehicles (Wang *et al.* 2016), bridges (Nguyen *et al.* 2022), and the analysis of physiological signals in brain imaging (Duff *et al.* 2008). Understanding the impact of vertical random vibrations during transport is essential, particularly in the context of growing e-commerce and food logistics. Field studies show that vibration intensity depends on road type, vehicle speed, and cargo position, with the highest PSD levels and most damage occurring in the upper layers of stacked loads (Berardinelli *et al.* 2003; Jarimopas *et al.* 2005). Previous studies in the literature have investigated the dynamic behavior of corrugated paperboard, with particular attention to the vibration damping performance of cushioning pads and the fatigue analysis of transport packaging (Guo *et al.* 2010; Wang *et al.* 2020). Corrugated board packaging combined with plastic foil has demonstrated better vibration damping and thermal insulation, helping preserve product quality in beer transport (Paternoster *et al.* 2017).

However, standard tests such as ASTM D7386-16 (2025) often fail to reflect real-world vibration spectrum, especially at low frequencies (Molnár *et al.* 2023). To address this, researchers have developed numerical models combining static compression, resonance analysis, and advanced finite element analysis (FEA) to predict packaging performance under dynamic loads (Mrówczyński *et al.* 2023; Cornaggia *et al.* 2024). These models, validated through experimental compression tests, have proven effective in predicting packaging failure modes and optimizing packaging design. Furthermore, FEA has also been used to evaluate energy absorption and bruise reduction in fresh produce packaging, showing that the use of double-layer corrugated board can reduce stress by over 30% in impact scenarios (Hafizh *et al.* 2024). A comprehensive review of standards, measurement techniques, and predictive models of noise and vibration was presented by Khan and Burdzik (2023).

In the pursuit of more sustainable packaging and transport systems, Life Cycle Assessment (LCA) has become an essential tool for evaluating the environmental performance of different packaging solutions. Studies consistently show that both material choices and packaging design significantly influence the total environmental impact throughout the life cycle of transport packaging. An example is the study by Kim *et al.* (2023b), which demonstrated that optimizing the interaction between pallet stiffness and corrugated box strength can lead to material savings and reduce environmental impacts, primarily by lowering the use of corrugated board.

Scientific advances in corrugated board engineering have also extended its durability and recyclability, supporting circular economy goals (Garbowski and Pośpiech 2024). Numerous studies, including life cycle assessments, have been conducted to identify the most optimal solutions in terms of material type, composition, and structural design (Chen *et al.* 2011; Wang *et al.* 2021; Zambujal-Oliveira and Fernandes 2024). In this context, corrugated board has been recognized as a promising material due to its recyclability and potential for emissions reduction, particularly when design optimization is applied (Jannes *et al.* 2023; Ketkale and Simske 2023; Chowdury and Kabir 2024). Broader comparative studies confirm that reusable systems, such as plastic crates, tend to

outperform single-use corrugated board in terms of long-term environmental and economic performance, despite their higher initial transport emissions or production inputs (Albrecht *et al.* 2013; Accorsi *et al.* 2022). Moreover, simplified assessments demonstrate that reusable plastic packaging can offer up to 75% lower environmental loads than conventional wooden pallet systems, especially when high reusability and transport efficiency are achieved (Lee and Xu 2004). These insights underline the critical role of life cycle thinking in packaging design, revealing that sustainability gains depend not only on material selection but also on packaging reuse rates, supply chain configuration and end-of-life strategies.

Current trends, such as the rapid growth of e-commerce, the need for sustainable material management, and increasing expectations for transport efficiency are driving an ongoing search for innovative corrugated packaging solutions that deliver both functional and environmental benefits. In this context, one notable example is the development of an optimized export packaging for Persian limes, where genetic algorithms and TRIZ methodology were combined to reduce material usage 28% without compromising vertical compression strength, while also introducing novel non-spatial features such as airflow control and internal friction (Aguilar-Lasserre *et al.* 2020). Empirical studies highlight that packaging design is not only important for material efficiency but also for product protection. Wang *et al.* demonstrated that inadequate structural constraints within packaging can significantly increase vibration-induced damage during transport (Wang *et al.* 2025). Moreover, other research shows that specific design shortcomings — such as insufficient cushioning, poor immobilisation of items, and inadequate padding against drop/shock events — correlate strongly with higher incidences of product failure and box damage in transit (Chonhencob and Singh 2025).

This paper presents an analysis of innovatively designed corrugated board packaging system that aims to increase resistance to random vertical vibrations occurring during transportation. The study focuses on the vertical load-bearing capacity under controlled vibration conditions for packaging with relatively low probability of being dropped. In the context of previous studies (Zhang *et al.* 2017), vertical vibrations are identified as a key factor contributing to the degradation of mechanical properties of packaging materials. Building on a design-focused approach, the present study aimed to experimentally evaluate 25 corrugated board packaging variants intended for e-commerce, differing in board structure, layer configuration, and surface finish. The designs were developed as modifications of commercially used packaging solutions, with the purpose of enhancing their mechanical performance during road transport and extending their functionality to enable rapid forming and closing. The novelty of the work lies in (i) integrating random vibration and compression testing under standardized conditions, and (ii) assessing innovative geometries (modified FEFCO 759 and 426) optimized for stacking stability and closure strength. Through standardized box compression and random vibration tests (ISO 12048 1994; ISO 13355 2016), the load bearing capacity of each variant was assessed before and after dynamic loading, offering insights into how design modifications can enhance performance under simplified transport conditions. The results contribute to the development of high-durability packaging tailored to the demands of today's supply chains.

EXPERIMENTAL

Workflow of the Study

This study presents research on specially designed packaging resistant to transport load conditions. The initiative to develop new designs arose from the need to replace the packaging currently used in the distribution of manually prepared FMCG sets with alternatives offering performance aspects including improved transport durability, an accelerated manual assembly process, increased protection against microbiological contamination, and greater standardization of the designs. Technical drawings of the original packaging on the basis of which the new packaging constructions were developed are presented on Fig. 1.

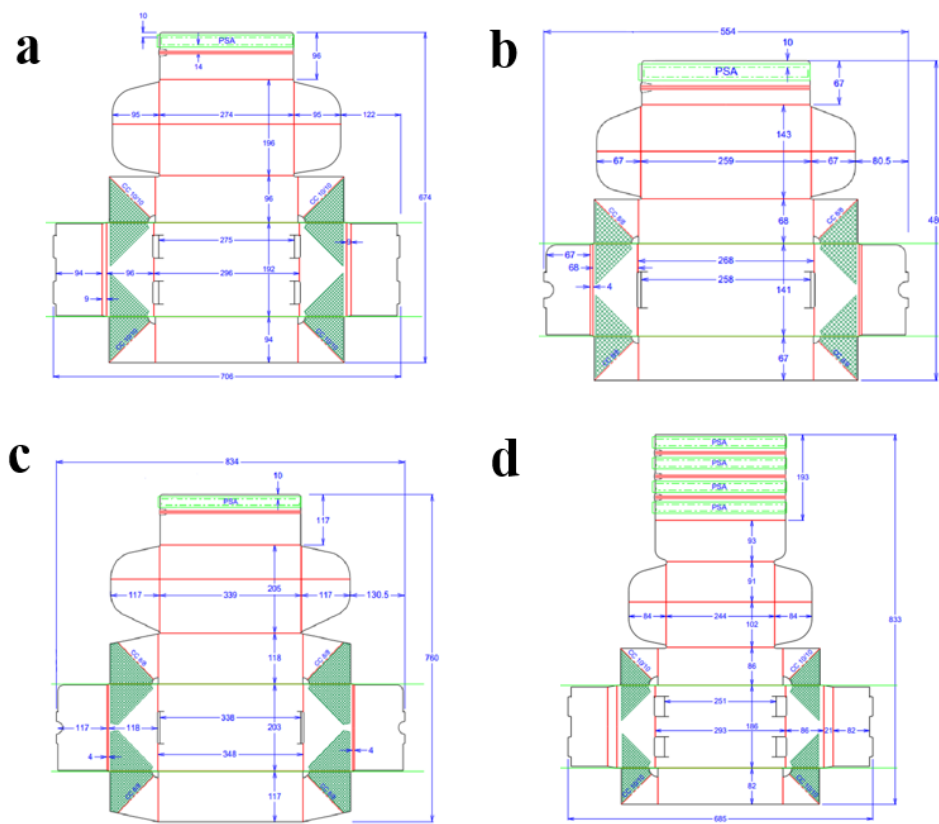


Fig. 1. Technical drawings of original packaging used on the market: (a) W1 300 × 200 × 100 mm, Flute E, B, C (b) W1 270 × 145 × 70 mm, flute E (c) W1 350 × 207 × 120 mm, (d) W2 300 × 200 × 100 mm flute EB, BC

The current study focuses on evaluating the resistance of newly designed packaging structures to random vertical vibrations occurring during transport. The experimental research program included a series of tests on 25 different types of packaging (see Fig. 2). Packaging was manufactured using converting machines - HQ flexographic printing machine, flatbed die-cutter, and a folder gluer. The study involved packages of three dimensions, which were the same as for original packaging: 300 × 200 × 100 mm, 270 × 145 × 70 mm, and 350 × 207 × 120 mm. Two specific packaging types labeled W1 (for E and B flute) and W2 (for C, EB and BC Flute) were used (see Fig. 3). The innovative nature

of W1 and W2 designs consists in reinforcing critical corner zones and lid–base interfaces through geometry modifications that increase double-wall regions without adding corrugated board mass. Compared to standard FEFCO structures, this approach enhances compressive resistance and dimensional stability during telescoping closure.

Packaging of W1 design is a modified FEFCO 759-type packaging—a self-locking, telescope-style lid-and-base combination. It contains a rectangular base panel with four vertical sidewalls, each incorporating integral corner flaps that fold inward and lock, creating double-thickness corners for stability. The top cover has a construction similar to the base but is slightly larger in plan dimensions so it can telescope over it. The elongated lid overlaps the base down to the bottom and includes pressure-sensitive adhesive and a tear tape to enable simple closure and easy opening.

Packaging of W2 design is a modified FEFCO 426-type packaging—a folder box with an integrated hinged lid. It contains a base panel, a rectangular bottom forming the main body of the box. A large upper flap is connected to the rear edge of the base *via* a continuous crease line and forms the integrated hinged lid. The sidewalls are vertical panels with locking flaps that rise to create the container walls. Small inner wings attached to the lid fold inward to reinforce the corners and protect the contents. The front closure flap is a tuck-in tab shaped to fit securely into the front wall opening, providing a neat, self-locking closure. For clarity, 3D visualization of folding of W2 type packaging was presented in Fig. 4.

Using FEFCO 759- and 426-types enables the possibility of introducing structural modifications in the form of additional adhesive areas, which are indicated on the grids as green fields with a mesh pattern (Fig. 3). Introducing such a modification facilitates folding and does not meaningfully increase die complexity. The only additional cost results from the extra adhesive used, which is negligible compared to the overall packaging cost and the potential gain in load-bearing capacity. An appropriately selected shape, size, and placement of the adhesive flaps enhance the bonding between adjacent walls, thereby preventing their displacement in uncontrolled directions during exposure to content vibrations. The dimensions and specific e-commerce scenarios were defined regarding the most frequently used types of e-commerce packaging.

Corrugated boards with E-, B-, and C-flutes were used, as well as double-walled boards EB-flute and BC-flute. The board supplier was Werner Kenkel Bochnia Ltd. The material properties, such as grammage, thickness, paper grammage and edge crush resistance (ECT), are presented in Table 1. The influence of coatings and varnishes was investigated for packages with dimensions of 300 × 200 × 100 mm. Three variants were tested: uncoated and unvarnished samples, samples with an aseptic coating, and samples with a varnish without active components.

Printing on corrugated boards constitutes an important approach for introducing new functionalities into packaging systems. However, printing process may lead to a localized reduction in the strength of corrugated board due to ink penetration and the mechanical impact of printing pressure on the fiber structure. The magnitude of this effect depends on process parameters such as roller hardness, ink viscosity, and the degree of sheet compression during printing, which can result in decreased resistance to crushing and compression. (Holmvall 2010; Yang and Christianson 2023)

Manual assembly process and hand-to-hand distribution of parcels considerably increases the risk of transmitting pathogenic microorganisms. In this study, the flexographic printing technique was employed to apply a thin antiseptic coating—a water-based varnish containing antimicrobial agents. The printing process involves the

application of pressure from the photopolymer plate onto the corrugated board surface to transfer a controlled amount of coating and to ensure layer continuity across the entire surface of the packaging. However, this process may adversely affect the integrity of the corrugated board structure. Moreover, one of the active components of the applied coating is a strong detergent, which can alter the paper's fibrous structure and weaken the starch-based adhesive bonds, consequently reducing the overall load-bearing capacity of the packaging.

Table 1. Material Parameters of Corrugated Boards Used in the Study

Corrugated board	Grammage (g/m ²)	Thickness (mm)	Papers grammage (g/m ²)	ECT (kN/mm)
E flute	374	1.55	120/95/125	3.9
B flute	387	2.95	125/95/125	4.2
C flute	537	4.15	170/135/170	6.0
EB flute	811	4.60	180/135/120/135/140	9.5
BC flute	1094	7.05	250/160/135/160/250	13.5

For each packaging type and board variant, 6 samples were prepared. Half of the samples (labeled as group A) were used to assess the compressive strength in a column compression test, known as the Box Compression Test (BCT). The results of these tests are referred to as BCT in this publication. The remaining samples (group B) were subjected to random vibration testing on vibration tables in accordance with standardized load protocols (ISO 13355 2016; ASTM D1469 2024). After vibration testing, a visual inspection was performed to document the condition and potential damage of the samples, accompanied by photographic documentation. In addition, samples from group B were subsequently tested in the BCT to evaluate the effect of vibration exposure on compressive strength; these results are referred to in this publication as BCT_V.

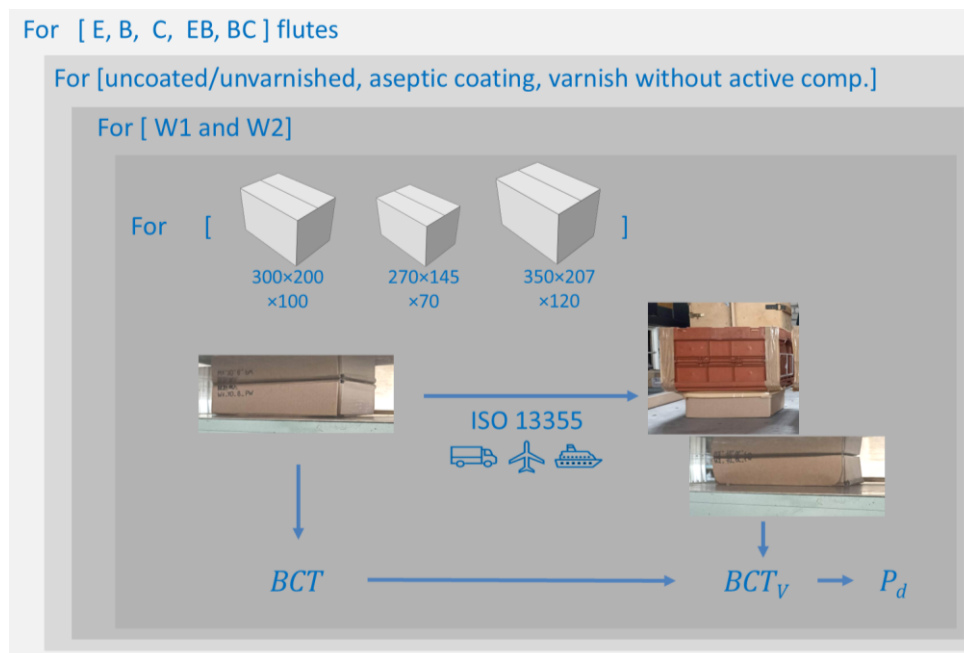


Fig. 2. Schematic overview of the study workflow with conceptual, not qualitative, displacements

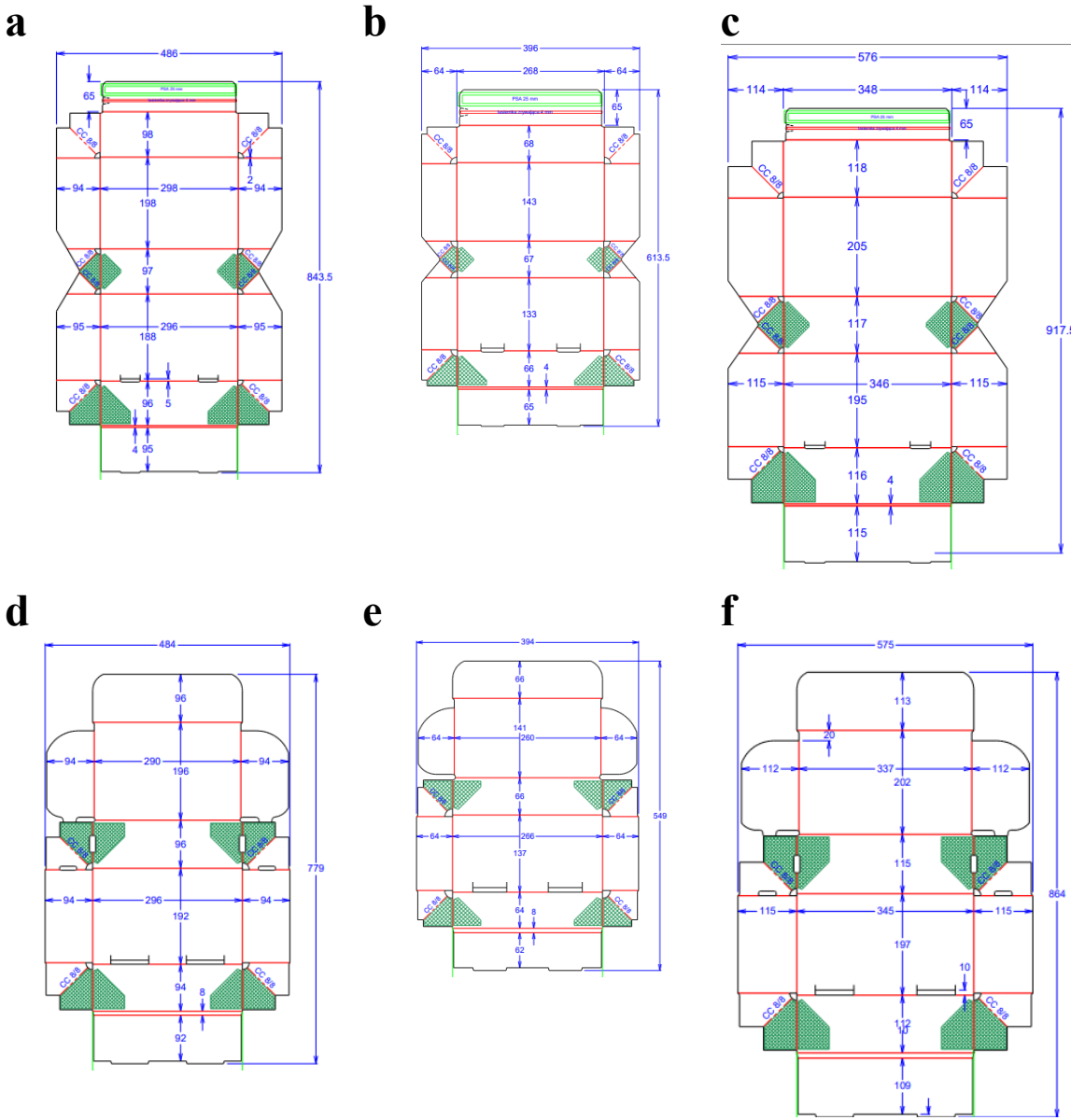


Fig. 3. Technical drawings of selected packaging: (a) W1 300 × 200 × 100 mm, (b) W1 270 × 145 × 70 mm, (c) W1 350 × 207 × 120 mm, (d) W2 300 × 200 × 100 mm, (e) W2 270 × 145 × 70 mm and (f) W2 350 × 207 × 120 mm

Experimental Setup

In this paper, the resistance to vertical vibrations occurring during transport was determined for different packaging designs. The procedure described in ISO 13355 (2016) for vertical random vibration testing of boxes was used. A sample of the corrugated board box, closed and fixed in the horizontal plane, was placed centrally on a rigid vibration table. The test setup is shown in Fig. 5.

Packaging used for hand-assembled FMCG sets distribution is often applied for products of various shapes and dimensions. Some of these products completely fill the internal space of the box, thereby contributing to load transfer, while others are packed loosely and do not support load-bearing.

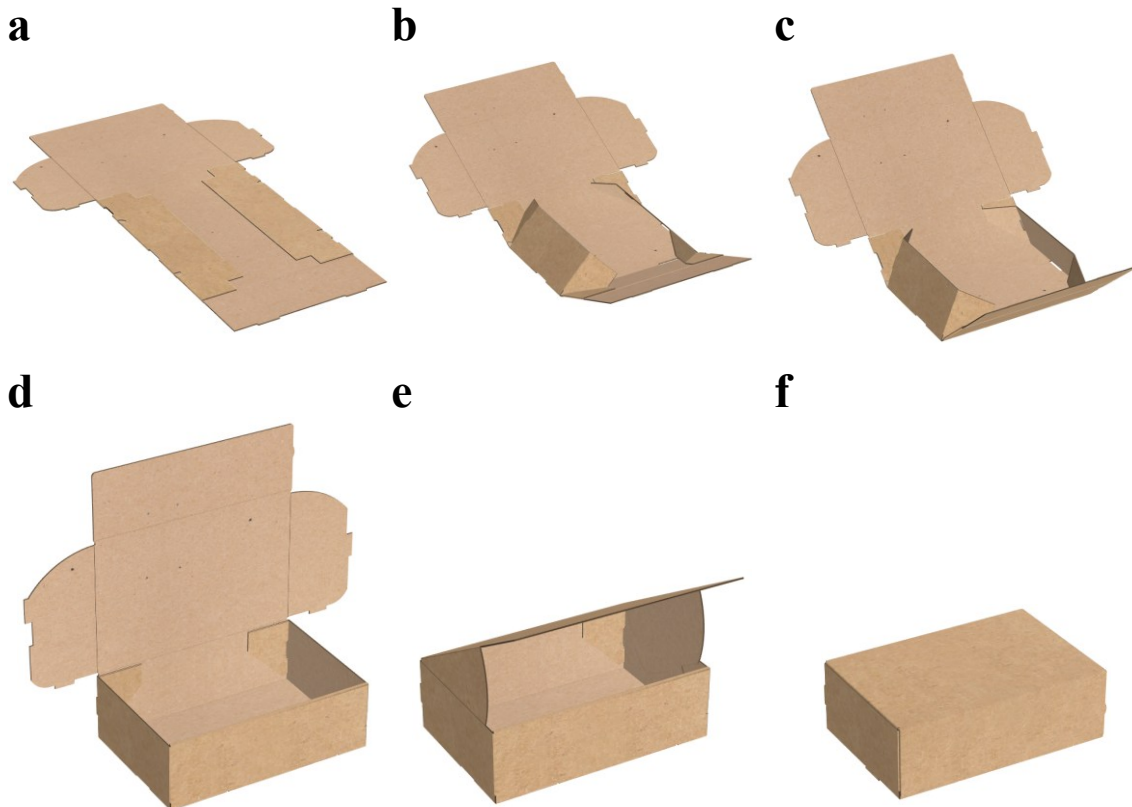


Fig. 4. 3D visualization of folding of W2 type packaging: (a) before folding, (b) raising the side walls, (c) locking the side walls, (d) folded box with open lid, (e) closing the lid, and (f) completely folded box



Fig. 5. Random vibration table test stand – L.A.B. Type HV88 from L.A.B. (Itasca, USA)

The purpose of the tests was to evaluate the strength of different packaging constructions, rather than to assess the performance of the entire transport system. Testing without internal contents eliminates the influence of the product, allowing the determination of the structural load-bearing capacity of the packaging itself— independent of the type or method of filling.

Test parameters, such as duration, temperature, relative humidity, and power spectral density (PSD), were previously defined. Random vibrations on the vibration table lasted 180 min and were conducted under laboratory conditions (temperature 23 °C and 50% relative humidity) (ISO 187 2022; TAPPI T402 sp-21 2021). Each reported BCT value represents the mean of twelve replicates. Standard deviations and coefficients of variation were calculated to assess data reproducibility. Statistical significance between groups (e.g., coating type, flute geometry) was tested using one-way analysis of variance (ANOVA) with a 95 % confidence level. Due to the lack of experimental data, the reference PSD values and test duration were adopted in accordance with the standard's guidelines (ISO 13355 2016), as shown in Fig. 6 and Table 2. The corrugated board boxes were conditioned for 24 h under laboratory conditions before the vertical random vibration test.

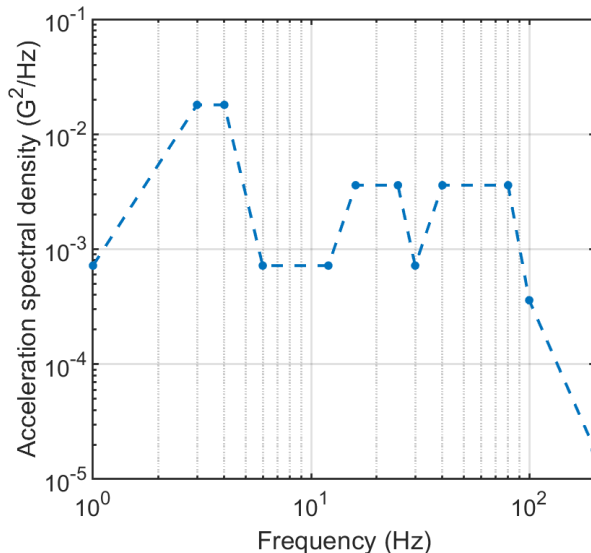


Fig. 6. Random vibration profile during packaging tests to reflect road transportation conditions

Table 2. Frequency-acceleration Data Used in the Power Spectral Density Profile

Frequency (Hz)	Acceleration Spectral Density (G ² /Hz)
1	0.00072
3	0.018
4	0.018
6	0.00072
12	0.00072
16	0.0036
25	0.0036
30	0.00072
40	0.0036
80	0.0036
100	0.00036
200	0.000018

Vertical random vibration tests were performed with a test load placed on the top surface of the packaging, simulating the stress of stacking packages during shipping. The test load value was calculated according to ASTM D4169-16 (2024) using Eq. 1,

$$L = M_f \cdot J \cdot \frac{l \cdot w \cdot h}{K} \cdot \frac{H - h}{h} \cdot F, \quad (1)$$

where L is the computed load; M_f is the shipping density factor; J is the mass correction factor; l , w , and h are the length, width, and height of the individual container, respectively; K is the volume correction factor; H is the maximum height of stack in transit vehicle; and F is the assurance level factor. In Table 3, the values of these parameters and the calculated test load for the three dimensions of the boxes are presented. Figure 7 shows a view of the packages with the equivalent load on the vibration table.

Table 3. Test Load Data for Vertical Random Vibration Protocol

Box (mm)	M_f (kg/m ³)	J (N/kg)	l (m)	b (m)	h (m)	K (m ³ /m ³)	H (m)	F (-)	L (N)
300×200×100	160	9.8	0.300	0.200	0.100	1	1.9	1	169.3
270×145×70	160	9.8	0.270	0.145	0.070	1	1.9	1	112.3
350×207×120	160	9.8	0.350	0.207	0.120	1	1.9	1	202.2



Fig. 7. Photos of the boxes during vertical vibration tests with equivalent load: (a) W1 samples and (b) W2 samples

The compression strength of corrugated board packaging was evaluated using the box compression test accordance to ISO 12048 (1994). The experiments were done in the laboratory on a Lorentzen & Wettre CT 100 press with a mechanical drive, equipped with two loading plates, of which one was displaced vertically to apply the compressive force to the box. The crosshead speed was set to 10 mm/min as specified in the standard. Prior to testing, the box samples were conditioned for 24 h at a temperature of 23 °C and relative humidity of 50% to ensure stabilization of material properties. During BCT measurements, the compressive force and the corresponding deformation were continuously registered until the loss of stability or failure of the sample occurred. Representative examples of the tested packaging placed in the BCT press are shown in Fig. 8.

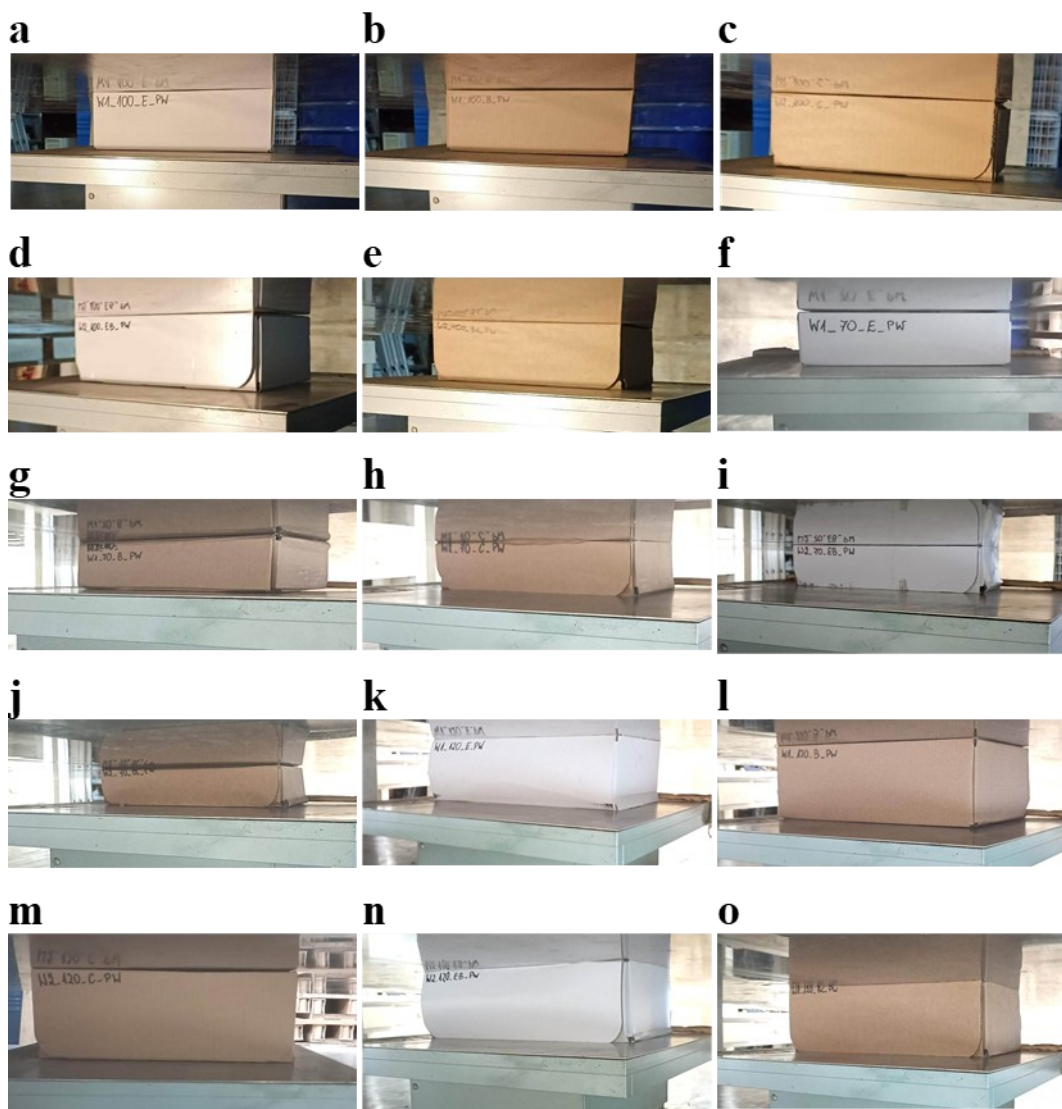


Fig. 8. Photographic documentation of conducting box compression tests: 300 × 200 × 100 box – (a) E flute, (b) B flute, (c) C flute, (d) EB flute; 270 × 145 × 70 box – (e) BC flute, (f) E flute, (g) B flute, (h) C flute, (i) EB flute, (j) BC flute; 350 × 207 × 120 box – (k) E flute, (l) B flute, (m) C flute, (n) EB flute, and (o) BC flute

RESULTS AND DISCUSSION

Compression Strength

As described earlier, the extended testing studies were performed to determine the decrease of BCT due to the influence of the simplified, simulated standardized vertical transport loading. Contrary to expectations, in several cases vibration exposure slightly increased the compressive strength. This effect may be attributed to partial micro-compaction of corrugated walls or better load redistribution after dynamic conditioning. From the mechanical point of view, adhesive flaps enhance the bonding between adjacent walls, thereby preventing their displacement in uncontrolled directions during exposure to content vibrations.

In Table 4 and 5 all results of average compression strengths of packaging are summarized with their counterpart standard deviations.

Table 4. Compression Strengths with Standard Deviations of Various Boxes Before and After Random Vibration Tests

No.	Type-dimensions	Flute	Finish	BCT (std. dev.) (kN)	BCT _v (std. dev.) (kN)	P _d (%)
1	W1 300×200×100	E	antiseptic coating	1.10 (0.02)	1.18 (0.02)	7.3
2	W1 300×200×100	B	antiseptic coating	1.54 (0.04)	1.61 (0.03)	4.5
3	W2 300×200×100	C	antiseptic coating	2.56 (0.06)	2.87 (0.11)	12.1
4	W2 300×200×100	EB	antiseptic coating	3.65 (0.05)	4.24 (0.29)	16.2
5	W2 300×200×100	BC	antiseptic coating	7.08 (0.34)	8.07 (0.11)	14
6	W1 300×200×100	E	no coating	1.02 (0.04)	1.24 (0.06)	21.6
7	W1 300×200×100	B	no coating	1.55 (0.03)	1.69 (0.15)	9
8	W2 300×200×100	C	no coating	2.62 (0.22)	3.11 (0.40)	18.7
9	W2 300×200×100	EB	no coating	4.07 (0.20)	4.22 (0.28)	3.7
10	W2 300×200×100	BC	no coating	7.00 (0.15)	8.05 (0.10)	15
11	W1 300×200×100	E	with varnish, without active ingr.	1.04 (0.02)	1.20 (0.02)	15.4
12	W1 300×200×100	B	with varnish, without active ingr.	1.57 (0.04)	1.58 (0.04)	0.6
13	W2 300×200×100	C	with varnish, without active ingr.	2.56 (0.03)	2.87 (0.11)	12.1
14	W2 300×200×100	EB	with varnish, without active ingr.	4.07 (0.13)	4.19 (0.03)	2.9
15	W2 300×200×100	BC	with varnish, without active ingr.	7.08 (0.20)	7.90 (0.31)	11.6
16	W1 270×145×70	E	antiseptic coating	0.97 (0.06)	1.05 (0.02)	8.2
17	W1 270×145×70	B	antiseptic coating	2.04 (0.15)	2.05 (0.20)	0.5
18	W2 270×145×70	C	antiseptic coating	2.94 (0.07)	3.03 (0.09)	3.1
19	W2 270×145×70	EB	antiseptic coating	4.25 (0.18)	4.24 (0.28)	-0.2
20	W2 270×145×70	BC	antiseptic coating	7.17 (0.31)	7.29 (0.14)	1.7
21	W1 350×207×120	E	antiseptic coating	1.10 (0.05)	1.30 (0.07)	18.2
22	W1 350×207×120	B	antiseptic coating	1.46 (0.10)	1.54 (0.08)	5.5
23	W2 350×207×120	C	antiseptic coating	2.18 (0.10)	2.93 (0.23)	34.4
24	W2 350×207×120	EB	antiseptic coating	3.49 (0.03)	4.51 (0.17)	29.2
25	W2 350×207×120	BC	antiseptic coating	8.79 (0.12)	9.47 (0.22)	7.7

Table 5. Compression Strengths with Standard Deviations for Preliminary Tests Before and After Exposition to Random Vibrations

No.	Type-dimensions	Flute	Finish	BCT (std. dev.) (kN)	BCT _v (std. dev.) (kN)	P _d (%)
1	W1 300×200×100	E	no coating	1.12 (0.09)	1.23 (0.18)	8.9
2	W1 300×200×100	B	no coating	1.34 (0.09)	1.56 (0.16)	14.1
3	W1 300×200×100	C	no coating	2.12 (0.16)	2.04 (0.23)	-3.8
4	W2 300×200×100	EB	no coating	2.61 (0.25)	2.80 (0.25)	6.8
5	W2 300×200×100	BC	no coating	2.57 (0.05)	2.75 (0.08)	6.5
6	W1 270×145×70	E	no coating	1.27 (0.10)	1.27 (0.36)	0.0
7	W1 350×207×120	E	no coating	1.10 (0.07)	1.18 (0.07)	6.8

For each case, the type of packaging (W1 or W2), dimensions (300 × 200 × 100 mm, 270 × 145 × 70 mm, or 350 × 207 × 120 mm), fluting type (E, B, C, EB, or BC), and finish variant (antiseptic coating, no coating or with varnish, without active ingredients) are presented. Additionally, the BCT column states for the strength received from A batch samples – not designated for random vibration tests, while the *BCT_v* column represents B batch samples, which are tested for determining its column-wise compression strength after random vibration testing. Both testing protocols, compressive strength tests, and random vibration tests were described in the “Experimental setup” section. Furthermore, percentage differences, *P_d*, of those data were computed according to Eq. 2 and presented in the last column of Table 4. Percentage differences, *P_d*, were color-coded, with the lowest values shown in red and the highest in green. Equation 2, given below, was used to calculate the percentage differences.

$$P_d = \frac{BCT_v - BCT}{BCT} \times 100\% \quad (2)$$

DISCUSSION

The results presented in Table 4 lead to practically relevant conclusions. The overall average increase in load-bearing capacity between cases tested before and after random vibration testing across all cases was 10.9%. This counterintuitive improvement in post-vibration strength could result from the closure of initial geometric imperfections and the stabilization of the flute–liner contact zones during dynamic excitation. Similar compaction effects were previously observed for lightweight corrugated panels under cyclic loading. To verify this hypothesis, future studies should include microscopic inspection or 3D scanning before and after testing.

Prior to the main series of tests presented in this study, a pilot assessment was performed on packaging types that had been used commercially up to now. Results of these tests are presented in Table 5. Seven cases with corrugated board variability (flutes E, B, C, EB, and BC) and dimensions of 300 × 200 × 100 mm, 270 × 145 × 70 mm, and 350 × 207 × 120 mm, comparable to the final designs, were selected. Their load-bearing capacity was measured before and after random vibration testing to determine the effect of applying transport loads. The changes in pilot studies resulted in 8.9%, 0%, 6.8%, 14.1%, -3.8% (a decrease), 6.8%, and 6.5% with a total average of 5.6%. These results indicate a clear increase while comparing the outcome of the study presented in the paper (total average of

10.9%) with the pilot series (5.6%), confirming that the innovative packaging designs demonstrate enhanced resistance to transport loads represented by standardized testing procedures. Apart from general observations, additional, more detailed conclusions can be drawn.

When considering the coating groups of corrugated board packaging, the mean increases in load-bearing capacity were 10.8% for group 1 (Table 4, cases 1 to 5), 13.6% for group 2 (Table 4, cases 6 to 10), and 8.5% for group 3 (Table 4, cases 11 to 15). No characteristic tendency was observed here. Additionally, results revealed that no unambiguous overall effect of the coating could be identified through case-to-case comparison. In fact, when antiseptic coating (cases 1 to 5) was taken as the reference, differences between uncoated cardboard packaging (cases 6 to 10) and coated with varnish, without active ingredients (cases 11 to 15) ranged from negative values (P_d for coated with antiseptic media is greater) to positive (P_d for coated with antiseptic media is lower) values.

Furthermore, when considering the dimension groups of corrugated board packaging, if group 1 (cases 1 to 5) would be the reference, the mean increases in load-bearing capacity were 2.7% for group 4 (Table 4, cases 16 to 20) and 19.0% for group 5 (Table 4, cases 20 to 25). Similarly, no characteristic trend could be observed in this case. Moreover, a case-to-case comparison of packaging dimensions also did not yield clear dependencies. Analysis of cases 1 to 5 (300 × 200 × 100 mm) and their counterparts, *i.e.*, cases 16 to 20 (270 × 145 × 70 mm) and 21 to 25 (350 × 207 × 120 mm) revealed no evident relationship between packaging size and the change in load-bearing capacity – the differences ranging from negative values (P_d for 300 × 200 × 100 mm packaging is greater) to positive (P_d for 300 × 200 × 100 mm packaging is lower). These cases regard packaging with antiseptic coating, further supporting the conclusion that the observed differences are not attributable to dimensional variation.

In the study, three packaging dimensions were tested, namely, 300 × 200 × 100 mm, 270 × 145 × 70 mm, and 350 × 207 × 120 mm. Due to simultaneous change of length, width, and height — it is not possible to isolate the effect of individual geometrical parameter. The experimental design was intended to compare realistic packaging configurations rather than controlled geometric variations. Therefore, the obtained results do not provide sufficient evidence to draw conclusions regarding the effect of a single dimension on the packaging's resistance to transport loads. The results reflect the combined influence of structural parameters, representing practical conditions rather than a strict single-factor design. The analysis of the influence of a single dimension on the packaging's resistance to transport loads was beyond the scope of this paper. Next, grouping the results by flute type also does not reveal consistent tendencies. The average values of BCT increase amounted to 14.1% for E-flute, 4.0% for B-flute, 16.1% for C-flute, 10.4% for EB-flute, and 10.0% for BC-flute. Again, no systematic trend is apparent and variations in flute height, which reflect changes in board stiffness, do not result in a consistent effect.

This study focuses on the evaluation of vertical load-bearing capacity under controlled vibration conditions. The obtained results should be interpreted as indicators of relative structural performance rather than as absolute measures of behavior under real-world operational conditions. Accordingly, the conclusions do not claim full representativeness of parcel delivery systems, but instead aim to support comparative assessment within the defined experimental framework. Moreover, observed effects are conditional, design-dependent, and limited to empty-box compression behavior. The detailed analysis is deferred to future work. Conversely, there are studies reporting the opposite effect, such as that of Jung and Park (2012).

While displacement-based metrics and post-peak behavior could provide deeper insight into the observed effects, such data were not recorded during the present experimental campaign. Nevertheless, it should be noted that structural compaction may occur beyond the initial buckling event, and that applied vibration may act as a pseudo-creep or mechanical conditioning process, leading to an apparent increase in measured strength. Importantly, an increased empty-box BCT does not necessarily translate into improved product protection. In particular, enhanced load-bearing capacity achieved at the expense of increased deformation may be detrimental for damage-sensitive contents, such as fresh produce.

As indicated by Rouillard *et al.* (2021), there are many approaches for laboratory simulation of transport vibration. ISO 13355 PSD-based vibration testing was selected to ensure repeatability, standard compliance, and comparability, while acknowledging that field-measured vibration spectra and ISTA protocols may better capture parcel delivery dynamics. Another limitation of the paper is that the vibration motion was not considered in all orientations, which is characteristic for testing e-commerce packaging.

Despite the limitations, the present findings indicate that innovative packaging designed for the study demonstrates a general tendency toward improved resistance to transport loads. The magnitude of this effect is highly dependent on specific material and design factors and no single parameter (such as analyzed design type, coating version, flute type, or packaging dimensions) can be identified as a dominant determinant.

CONCLUSIONS

1. Modified packaging designs show a clear improvement in resistance to transport loads, as evidenced by an average increase in load-bearing capacity of 10.9% after vibration testing — more than twice as high as in the preliminary studies. The greatest changes in load capacity after vibration were observed for the largest boxes, mainly for wave C and EB. This suggests that the applied design solutions effectively enhance the stability of the packaging during transport. However, because this effect is counterintuitive, it should be further investigated and confirmed by additional research studies, for instance by applying alternative laboratory simulations of transport vibrations.
2. The observed increase in strength after vibration likely results from compaction of the corrugated board structure, including the elimination of initial geometric imperfections and stabilization of the flute–liner contact. This mechanism has previously been observed in other lightweight layered structures subjected to cyclic loading.
3. Analysis of the effects of coatings, dimensions, and flute types did not reveal clear trends or dominant factors that could systematically determine changes in load-bearing capacity after vibration. Differences between cases were variable, both positive and negative, indicating a complex and multifactorial nature of the structural response.

ACKNOWLEDGEMENTS

Funding

The work uses the results of research carried out as part of the project implemented by the company WERNER KENKEL Bochnia Spółka z o. o. The project was funded within the grant of The National Centre for Research and Development under the number POIR.01.01.01-00-0002/21.

REFERENCES

Accorsi, R., Battarra, I., Guidani, B., Manzini, R., Ronzoni, M., and Volpe, L. (2022). “Augmented spatial LCA for comparing reusable and recyclable food packaging containers networks,” *J. Clean. Prod.* 375, article 134027. <https://doi.org/10.1016/j.jclepro.2022.134027>

Aguilar-Lasserre, A. A., Torres-Sánchez, V. E., Fernández-Lambert, G., Azzaro-Pantel, C., Cortes-Robles, G., and Román-del Valle, M. A. (2020). “Functional optimization of a Persian lime packing using TRIZ and multi-objective genetic algorithms,” *Comput. Ind. Eng.* 139, article 105558. <https://doi.org/10.1016/j.cie.2018.12.005>

Albrecht, S., Brandstetter, P., Beck, T., Fullana-i-Palmer, P., Grönman, K., Baitz, M., Deimling, S., Sandilands, J., and Fischer, M. (2013). “An extended life cycle analysis of packaging systems for fruit and vegetable transport in Europe,” *Int. J. Life Cycle Assess.* 18, 1549-1567. <https://doi.org/10.1007/s11367-013-0590-4>

Annibal, S., Dubecq, E., and Nolot, J. B. (2023). “Impact of shocks and vibrations on strawberry quality in the supply chain, according to packaging,” *Acta Hortic.* 1364, 375-382. <https://doi.org/10.17660/ActaHortic.2023.1364.48>

Archaviboonyobul, T., Chaveesuk, R., Singh, J., and Jinkarn, T. (2020). “An analysis of the influence of hand hole and ventilation hole design on compressive strength of corrugated fiberboard boxes by an artificial neural network model,” *Packag. Technol. Sci.* 33, 171-181. <https://doi.org/10.1002/pts.2495>

ASTM D4169 (2024). “Standard practice for performance testing of shipping containers and systems,” ASTM International, West Conshohocken, PA, USA.

ASTM D7386-16 (2025). “Standard practice for performance testing of packages for single parcel delivery systems,” ASTM International, West Conshohocken, PA, USA.

Berardinelli, A., Donati, V., Giunchi, A., Guarneri, A., and Ragni, L. (2003). “Effects of transport vibrations on quality indices of shell eggs,” *Biosyst. Eng.* 86, 495-502. <https://doi.org/10.1016/j.biosystemseng.2003.08.017>

Çakmak, B., Alayunt, F., Akdeniz, C., Can, Z., and Aksoy, U. (2010). “Assessment of the quality losses of fresh fig fruits during transportation,” *J. Agr. Sci.-Tarim Bili.* 16, 180-193. https://doi.org/10.1501/Tarimbil_0000001137

Chen, J., Zhang, Y., and Sun, J. (2011). “An overview of the reducing principle of design of corrugated box used in goods packaging,” *Proc. Environ. Sci.* 10, 992-998. <https://doi.org/10.1016/j.proenv.2011.09.159>

Chonhenchob, V., and Singh, S. P. (2025). “A comparison of corrugated boxes and reusable plastic containers for mango distribution,” *Packag. Technol. Sci.* 16, 231-237. <https://doi.org/10.1002/pts.630>

Chowdhury, T., and Kabir, G. (2024). "Lifecycle assessment (LCA) of package deliveries: Sustainable decision-making for the academic institutions," *Green and Low-Carbon Economy* 2, 1-13. <https://doi.org/10.47852/bonviewGLCE3202824>

Cornaggia, A., Mrówczyński, D., Gajewski, T., Knitter-Piątkowska, A., and Garbowski, T. (2024). "Advanced numerical analysis of transport packaging," *Appl. Sci.* 14, article 11932. <https://doi.org/10.3390/app142411932>

Duff, E. P., Johnston, L. A., Xiong, J., Fox, P. T., Mareels, I., and Egan, G. F. (2008). "The power of spectral density analysis for mapping endogenous BOLD signal fluctuations," *Hum. Brain Mapp.* 29, 778-790. <https://doi.org/10.1002/hbm.20601>

Fadiji, T., Ambaw, A., Coetzee, C. J., Berry, T. M., and Opara, U. L. (2018). "Application of finite element analysis to predict the mechanical strength of ventilated corrugated paperboard packaging for handling fresh produce," *Biosyst. Eng.* 174, 260-281. <https://doi.org/10.1016/j.biosystemseng.2018.07.014>

Fadiji, T., Coetzee, C. J., and Opara, U. L. (2016). "Compression strength of ventilated corrugated paperboard packages: Numerical modelling, experimental validation and effects of vent geometric design," *Biosyst. Eng.* 151, 231-247. <https://doi.org/10.1016/j.biosystemseng.2016.09.010>

Fahmy, K., and Nakano, K. (2013). "Favorable transportation conditions preventing quality loss of 'jiro' persimmon for exports," *Acta Hortic.* 1011, 73-80. <https://doi.org/10.17660/ActaHortic.2013.1011.7>

Fehér, L., Pidl, R., and Böröcz, P. (2023). "Creep behaviour of day-old chicken corrugated paperboard packaging under different uniaxial compression loads: An experimental study," *Packag. Technol. Sci.* 37, 51-63. <https://doi.org/10.1002/pts.2780>

Garbowski, T. (2023a). "Evaluating safety factors in corrugated packaging for extreme environmental conditions," *Packag. Rev.* 4, 6-15. <https://doi.org/10.15199/42.2023.4.1>

Garbowski, T. (2023b). "Safety factors in the design of corrugated board packaging," *Packag. Rev.* 3, 16-22. <https://doi.org/10.15199/42.2023.3.2>

Garbowski, T., and Pośpiech, M. (2024). "The impact of scientific research on corrugated board on the lifecycle of packaging," *Packag. Rev.* 4, 6-17. <https://doi.org/10.15199/42.2024.4.1>

Guo, Y., Xu, W., Fu, Y., and Zhang, W. (2010). "Comparison studies on dynamic packaging properties of corrugated paperboard pads," *Engineering* 2, 378-386. <https://doi.org/10.4236/eng.2010.25049>

Hafizh, M., Mecheter, A., Tarlochan, F., and Pathare, P. B. (2024). "Evaluation of bruising susceptibility and response of pears under impact loading through finite element analysis," *Appl. Sci.* 14, article 2490. <https://doi.org/10.3390/app14062490>

Holmvall, M. (2010). *Nip Mechanics, Hydrodynamics and Print Quality in Flexo Post-Printing*, PhD Dissertation. Mid Sweden University, Sweden

ISO 187 (2022). "Paper, board and pulps—Standard atmosphere for conditioning and testing and procedure for monitoring the atmosphere and conditioning of samples," International Organization for Standardization, Geneva, Switzerland.

ISO 12048 (1994). "Packaging—Complete, filled transport packages—Compression and stacking tests using a compression tester," International Organization for Standardization, Geneva, Switzerland.

ISO 13355 (2016). "Packaging—Complete, filled transport packages and unit loads—Vertical random vibration test," International Organization for Standardization, Geneva, Switzerland.

Jannes, R., Vanhauwermeiren, P., Slaets, P., and Juwet, M. (2023). "Assessing the sustainable potential of corrugated board-based bundle packaging of PET bottles: A life cycle perspective—A case study," *Clean Technol.* 5(4), 1214-1234. <https://doi.org/10.3390/cleantechol5040061>

Jarimopas, B., Singh, S. P., and Saengnil, W. (2005). "Measurement and analysis of truck transport vibration levels and damage to packaged tangerines during transit," *Packag. Technol. Sci.* 18, 179-188. <https://doi.org/10.1002/pts.687>

Jung, H. M., and Park, J. G. (2012). "Effects of vibration fatigue on compression strength of corrugated fiberboard containers." *Journal of Biosystems Engineering* 37(1), 51-57.

Ketkale, H., and Simske, S. (2023). "A life cycle analysis and economic cost analysis of corrugated cardboard box reuse and recycling in the United States," *Resources* 12(2), article 22. <https://doi.org/10.3390/resources12020022>

Khan, D., and Burdzik, R. (2023). "Measurement and analysis of transport noise and vibration: A review of techniques, case studies, and future directions," *Measurement* 220, article 113354. <https://doi.org/10.1016/j.measurement.2023.113354>

Kim, S., Horvath, L., Molina, E., Frank, B., Johnson, S., and Johnson, A. (2023a). "Predicting the effect of pallet overhang on the box compression strength," *Packag. Technol. Sci.* 36, 927-939. <https://doi.org/10.1002/pts.2768>

Kim, S., Horvath, L., Russell, J. D., and Park, J. (2023b). "Sustainable and secure transport: Achieving environmental impact reductions by optimizing pallet-package strength interactions during transport," *Sustainability* 15, article 12687. <https://doi.org/10.3390/su151712687>

Lee, S. G., and Xu, X. (2004). "A simplified life cycle assessment of re-usable and single-use bulk transit packaging," *Packag. Technol. Sci.* 17, 67-83. <https://doi.org/10.1002/pts.643>

Market Growth Reports (2023). "Corrugated cardboard market size, share, growth, and industry analysis, by type (single-wall corrugated, double-wall corrugated, triple-wall corrugated, recycled cardboard), by application (packaging, shipping, food & beverage, e-commerce, retail, moving & storage), Regional Insights and Forecast to 2033," Available online: <https://www.marketgrowthreports.com/market-reports/corrugated-cardboard-market-113178>, Accessed 26 Nov 2025.

Molnár, B., Németh, Z., Koltai, L., and Böröcz, L. (2023). "Comparison of field and standard random vibration for small-sized and stacked shipments during parcel delivery," *J. Test. Eval.* 51, 3745-3756. <https://doi.org/10.1520/JTE20220490>

Mrówczyński, D., Gajewski, T., and Garbowski, T. (2023). "A Simplified dynamic strength analysis of cardboard packaging subjected to transport loads," *Materials* 16, article 5131. <https://doi.org/10.3390/ma16145131>

Mrówczyński, D., Gajewski, T., Cornaggia, A., and Garbowski, T. (2024a). "Impact of temperature and humidity on key mechanical properties of corrugated board," *Appl. Sci.* 14, article 12012. <https://doi.org/10.3390/app142412012>

Mrówczyński, D., Gajewski, T., Pośpiech, M., and Garbowski, T. (2024b). "Estimation of the compressive strength of cardboard boxes including packaging overhanging on the pallet," *Appl. Sci.* 14, article 819. <https://doi.org/10.3390/app14020819>

Nguyen, T. Q., Nguyen, T. A., and Nguyen, T. T. (2022). "PSD characteristics for the random vibration signals used in bridge structural health monitoring in Vietnam based on a multi-sensor system," *Int. J. Distrib. Sens. Netw.* 18, article 15501329221125110. <https://doi.org/10.1177/15501329221125110>

Paternoster, A., Van Camp, J., Vanlanduit, S., Weeren, A., Springael, J., and Braet, J. (2017). "The performance of beer packaging: Vibration damping and thermal insulation," *Food Packag. Shelf Life* 11, 91-97. <https://doi.org/10.1016/j.fpsl.2017.01.004>

Rouillard, V., Lamb, M. J., Lepine, J., Long, M., and Ainalis, D. (2021). "The case for reviewing laboratory-based road transport simulations for packaging optimization," *Packag. Technol. Sci.* 34, 339-351. <https://doi.org/10.1002/pts.2563>

Sonnenberg, S. A. J., Rocha, J., Misol, M., and Rose, M. (2018). "Experimental validation of an acceleration power spectral density aircraft panel model given different excitations," *Can. Acoust.* 46, 19-30.

TAPPI T402 sp-21 (2021). "Standard conditioning and testing atmospheres for paper, board, pulp handsheets, and related products," TAPPI Press, Peachtree Corners, GA, USA.

Wang, C.-C., Chen, C.-H., and Jiang, B. C. (2021). "Shock absorption characteristics and optimal design of corrugated fiberboard using drop testing," *Appl. Sci.* 11, article 5815. <https://doi.org/10.3390/app11135815>

Wang, L., Xie, Z., Wu, Y., Gao, J., and Song, H. (2025). "Effects of packaging constraints on vibration damage of 'Huangguan' pear during simulated transport," *Horticulturae* 11(7), article Number 749. <https://doi.org/10.3390/horticulturae11070749>

Wang, L., Zhao, Y., Li, L., and Ding, Z. (2016). "Research on the vibration characteristics of the commercial-vehicle cabin based on experimental design and genetic algorithm," *J. Vibroengineering* 18, 4664-4677. <https://doi.org/10.21595/jve.2016.17161>

Wang, L.-J., Lai, Y.-Z., and Wang, Z.-W. (2020). "Fatigue failure and Grms-N curve of corrugated paperboard box," *J. Vib. Control* 26, 1028-1041. <https://doi.org/10.1177/1077546319891322>

Yang, L., and Christianson, H. (2023). "A static compression study on the lateral pressure variations of flexo post-print on corrugated board," in: *Advances in Printing and Media Technology*, Vol. XLIX(IX) – Session 2A, 2-7, https://doi.org/10.14622/Advances_49_2023_02

Zambujal-Oliveira, J., and Fernandes, C. (2024). "The contribution of sustainable packaging to the circular food supply chain," *Packag. Technol. Sci.* 37, 443-456. <https://doi.org/10.1002/pts.2802>

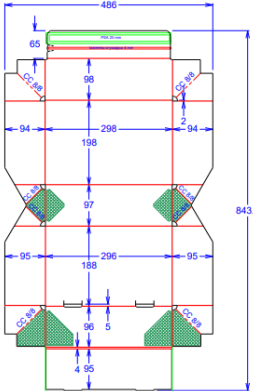
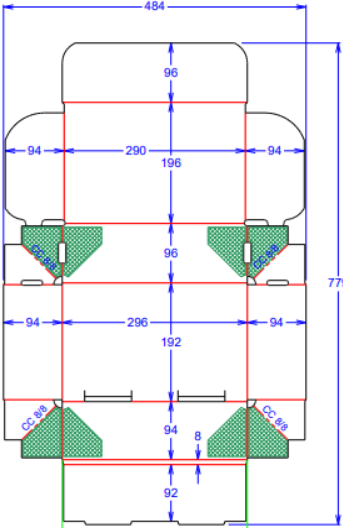
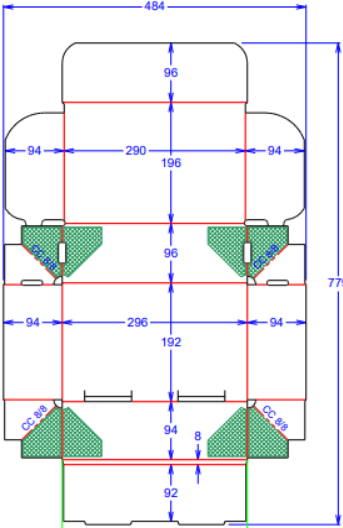
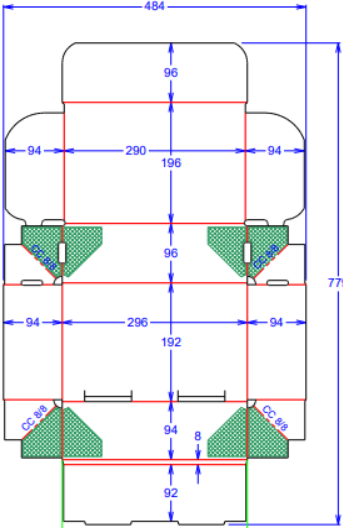
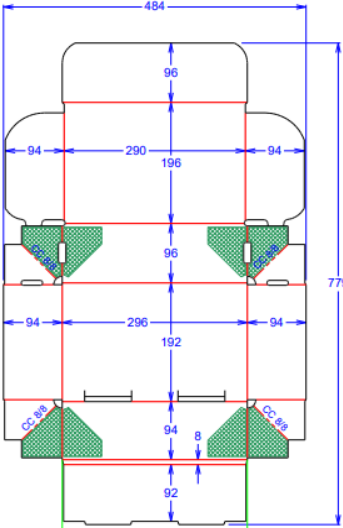
Zhang, Q., Saito K., and Nagaoka, K. (2017). "Damping package design using structural corrugated board," *Journal of Applied Packaging Research JAPR*, <https://repository.rit.edu/japr/vol9/iss3/2/>

Article submitted: December 6, 2025; Peer review completed: December 27, 2025;
Revised version received: January 20, 2021; Accepted: January 21, 2026; Published:
January 23, 2026.

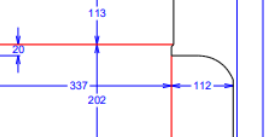
DOI: 10.15376/biores.21.1.2229-2253

APPENDIX

Appendix 1. Variants of Tested Packaging

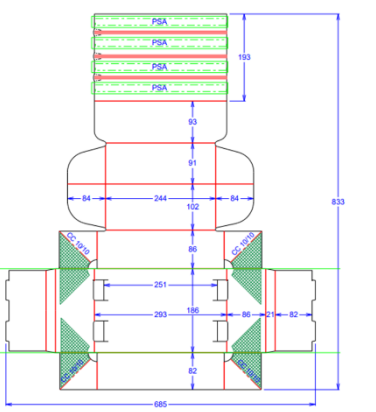
 W1 300 x 200 x 100mm	<ul style="list-style-type: none"> Flute: E ECT: 3,9k/Nm Grammage: 374 g/m² Thickness: 1,55mm Paper composition: 120/95/125 	No coating
		With varnish
		With antiseptic coating
 W2 300x200x100mm	<ul style="list-style-type: none"> Flute: B ECT: 4,2k/Nm Grammage: 387 g/m² Thickness: 2,95mm Paper composition: 125/95/125 	No coating
		With varnish
		With antiseptic coating
 W2 300x200x100mm	<ul style="list-style-type: none"> Flute: C ECT: 6,0k/Nm Grammage: 537g/m² Thickness: 4,15mm Paper composition: 170/135//170 	No coating
		With varnish
		With antiseptic coating
 W2 300x200x100mm	<ul style="list-style-type: none"> Flute: EB ECT: 9,5k/Nm Grammage: 811 g/m² Thickness: 4,60mm Paper composition: 180/135/120/135/140 	No coating
		With varnish
		With antiseptic coating
 W2 300x200x100mm	<ul style="list-style-type: none"> Flute: BC ECT: 13,5k/Nm Grammage: 1094 g/m² Thickness: 7,05mm Paper composition: 250/160//135/160/250 	No coating
		With varnish
		With antiseptic coating

<p>W1 270x145x70mm</p>		<ul style="list-style-type: none"> Flute: E ECT: 3,9k/Nm Grammage: 374 g/m² Thickness: 1,55mm Paper composition: 120/95/125 	With antiseptic coating
<p>W1 270x145x70mm</p>		<ul style="list-style-type: none"> Flute: B ECT: 4,2k/Nm Grammage: 387 g/m² Thickness: 2,95mm Paper composition: 125/95/125 	With antiseptic coating
<p>W2 270x145x70mm</p>		<ul style="list-style-type: none"> Flute: C ECT: 6,0k/Nm Grammage: 537g/m² Thickness: 4,15mm Paper composition: 170/135/170 	With antiseptic coating
<p>W2 270x145x70mm</p>		<ul style="list-style-type: none"> Flute: EB ECT: 9,5k/Nm Grammage: 811 g/m² Thickness: 4,60mm Paper composition: 180/135/120/135/140 	With antiseptic coating
<p>W2 270x145x70mm</p>		<ul style="list-style-type: none"> Flute: BC ECT: 13,5k/Nm Grammage: 1094 g/m² Thickness: 7,05mm Paper composition: 250/160//135/160/250 	With antiseptic coating
<p>W1 350x207x120mm</p>		<ul style="list-style-type: none"> Flute: E ECT: 3,9k/Nm Grammage: 374 g/m² Thickness: 1,55mm Paper composition: 120/95/125 	With antiseptic coating
<p>W1 350x207x120mm</p>		<ul style="list-style-type: none"> Flute: B ECT: 4,2k/Nm Grammage: 387 g/m² Thickness: 2,95mm Paper composition: 125/95/125 	With antiseptic coating

	<ul style="list-style-type: none"> Flute: C ECT: 6,0k/Nm Grammage: 537g/m² Thickness: 4,15mm Paper composition: 170/135//170 	With antiseptic coating
	<ul style="list-style-type: none"> Flute: EB ECT: 9,5k/Nm Grammage: 811 g/m² Thickness: 4,60mm Paper composition: 180/135/120/135/140 	With antiseptic coating
W2 350x207x120mm	<ul style="list-style-type: none"> Flute: BC ECT: 13,5k/Nm Grammage: 1094 g/m² Thickness: 7,05mm Paper composition: 250/160//135/160/250 	With antiseptic coating

Appendix 2. Variants of Packaging Used on the Market

		<ul style="list-style-type: none"> • Flute: E • ECT: 3,9k/Nm • Grammage: 351 g/m² • Thickness: 1,55mm • Paper composition: 125/95/100 	No coating
		<ul style="list-style-type: none"> • Flute: B • ECT: 4,2k/Nm • Grammage: 387 g/m² • Thickness: 2,95mm • Paper composition: 125/95/125 	No coating
		<ul style="list-style-type: none"> • Flute: C • ECT: 5,0/Nm • Grammage: 450 g/m² • Thickness: 4,15mm • Paper composition: 125/135/125 	No coating
W1	300x200x100mm		
		<ul style="list-style-type: none"> • Flute: E • ECT: 3,9k/Nm • Grammage: 351 g/m² • Thickness: 1,55mm • Paper composition: 125/95/100 	No coating
W1	270x145x70mm		
		<ul style="list-style-type: none"> • Flute: E • ECT: 3,9k/Nm • Grammage: 351 g/m² • Thickness: 1,55mm • Paper composition: 125/95/100 	No coating
W1	350x207x120mm		

 W2	300x200x100mm	<ul style="list-style-type: none">• Flute: EB• ECT: 9,5k/Nm• Grammage: 591 g/m²• Thickness: 4,60mm• Paper composition: 125/95/80/95/125	No coating
			<ul style="list-style-type: none">• Flute: BC• ECT: 7,0k/Nm• Grammage: 628g/m²• Thickness: 7,05mm• Paper composition: 135/95/80/95/135